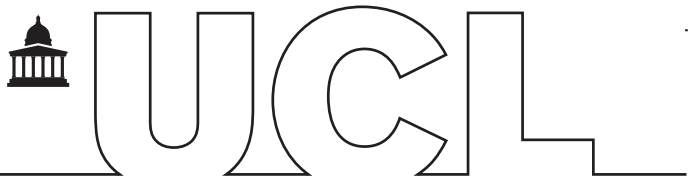

University College London

UCL PhD Upgrade Report

Qubit Coherence and Control

Author:
David F. Wise

Supervisor:
Prof. John Morton

Submitted in partial fulfilment for the degree of **MRes Quantum Technologies**

March 3, 2018

Abstract

Scientific documents often use LaTeX for typesetting. While numerous packages and templates exist, it makes sense to create a new one. Just because.

Contents

List of Figures

1 Introduction

At midnight all the agents and superhuman crew come out and round up everyone that knows more than they do

---

Quantum computing has been an active field of research since the concept was first suggested by Richard Feynman in the early 1980s [10]. Originally proposed as an efficient method for simulating chemical processes (something that traditional computers find extremely taxing) the discovery of several algorithms offering significant speed increases over classical computers has further fueLled research [26, 27]. Strong initial scepticism abounded regarding the potential for quantum computers to exist in the real world, primarily due to the concerns that error correction with such a complex device would be impossible[22]. This pessimism gave way with the identification of an error threshold for quantum computation. Given an error rate below a critical threshold it was possible to perform an arbitrarily long computation with negligible possibility of significant error [1, 25]. Following these discoveries serious attention has been given to the development of error correcting codes that might be implemented to allow a physical quantum computer to be *fault tolerant*.

Gottesman identified the class of error correcting codes known as *stabilizer codes*, where codes are defined by the group of logical operators that leave the code unchanged [13]. This class of quantum error correcting codes have become the dominant form in theoretical research. Of these one in particular has become the focus of much of the ongoing research of quantum computing, *the surface code*, developed by Bravyi and Kitaev [5]. Although other quantum error correcting codes (such as colour codes [31]) exist, the surface code has become the focus for experimental implementations. This is due mainly to the relatively high error threshold that it is able to tolerate, $\sim 0.5\%$, and the simple architecture of a planar grid of qubits.

In recent years there has been rapid progress in the development of physical qubits. Groups in both the academic and private sectors have shown small numbers of qubits functioning with error rates above the fault tolerant threshold [4, 23]. The successful recent approaches

have tended to focus on superconducting circuits to produce their qubits. Whilst these have proved excellent for the small numbers of qubits currently in use, it is likely that they will present significant additional challenges when scaling to numbers sufficient for useful, fault-tolerant quantum computation. With the numbers required likely to be close to 100×10^6 and the current size of these qubits close to 1mm^2, it will likely be impossible to use these qubits in their current form in a fault-tolerant quantum computer.
Although there are many alternative systems that could provide a qubit, this paper will focus on the use of the spins of nuclei and electrons bound to donors in semiconductors, particularly silicon. A seminal paper by Kane [15] stimulated much of the research interest in this field. He proposed using the spin of phosphorus nuclei in silicon as qubits with the ability to mediate interactions between neighbouring donor nuclei using the interaction between the electrons bound to each. These types of qubit are attractive due to their exceptionally long coherence times, the time that the qubit reliably stores quantum information for. A long coherence time relative to qubit gate times is essential, as this determines the error rate of the qubits. Coherence times as long as several seconds have been reported for donor spin qubits in silicon, whilst gate times can be as low as several nanoseconds [33]. Despite these advantages, development of these types of qubits for quantum computers has lagged behind the superconducting and ion trap versions [2]. This is due to the difficulty of isolating and addressing single donors in a silicon lattice. Kane's proposal required sub nano-metre precision in qubit placement to facilitate inter-qubit interactions. Even if this precision were achieved there remains the issue of how the requisite control circuitry could be integrated into such a dense design. This has lead to the development of more modern proposals to both overcome these difficulties and also to implement surface code based error correction.

One such proposal is from O'Gormann et al [19]. This proposal takes a similar approach to Kane, with qubits being donor spins in a silicon lattice. Where it differs significantly is in its use of two lattices of qubits. One of these is for the storage of data, whilst the other performs measurements on these data qubits. This measurement stage is placed above the data stage and held close, within 40nm, and moved in a repeating cycle over the data qubits. This allows each measurement qubit to perform $\hat{X}$ or $\hat{Z}$ measurement on groups of four data qubits, the stabilizer measurements that make up the fundamental units of surface code. This architecture allows for data qubits to be placed much farther apart - since no direct interaction between them is required. Several key research questions remain:

1. What donor species should be used for both types of qubit?

2. How are the measurement qubits to be read out?

3. How are the qubits to be controlled?

Whilst donors in silicon make excellent choices for the data qubits due to the properties stated above, a different qubit species is required for the measurement qubits to avoid an unwanted exchange interaction between the two lattices. Optical qubit readout is suggested in the proposal by O'Gormann et al and is a well studied means of reading the state of spin qubits, particularly in nitrogen-vacancy (NV) centres in diamond [16]. A concern with optical readout is the impact that illumination can have on the coherence times of donors in silicon. Silicon has a band gap energy equivalent to approximately 1058nm or photon energy of 1.17eV. Illumination at shorter wavelengths than this will create free electrons in the silicon conduction band. These can scatter off the electrons bound to donors, causing them to relax and shortening the T_1 time of the qubits as a whole [**Ross2017**]. NV centres are read out at between 500nm and 600nm, illumination that would reduce data qubit coherence times and increase the qubit error rate. Alternative optically addressed spin qubits at higher wavelengths exist, such as the di-vacancy centre in silicon carbide [7], but a vital question is what wavelengths can be used for read-out without compromising data qubit coherence times. This report addresses this question by examining the effect of various laser wavelengths close to the silicon band gap on the coherence times of electrons bound to phosphorus donors in silicon.

Another key question presented by the O'Gormann proposal is how to control the data qubits. The frequencies traditionally used for electron spin resonance are between 8GHz and 10GHz. Electromagnetic radiation at these frequencies require large coaxial cables and cavities for transmission. This makes it almost impossible to individually address qubits using microwaves. Instead the solution proposed by Kane is to use global microwave pulses, addressing all qubits at once. To selectively control qubits the DC Stark shift can be employed - DC electric fields can be used to shift the electron spin transition frequency meaning that a global microwave field will not effect them. Unlike RF radiation, DC signals are easily multiplexed and the commercial electronics industry has achieved fabrication precision well within that required by the O'Gormann proposal. The stark shift of donors in silicon has been well studied but has yet to be quantified in certain systems [21]. Among these is the hyperfine interaction between the donor electron and the silicon-29 nuclei present in natural silicon. The nuclear bath has been identified as a potential quantum register and the ability to tune the interaction between data qubits and memory could be of use.

2 Theory

2.1 Electron Spin Resonance

2.1.1 Background Theory

Electron spin resonance (EPR) functions by detecting the energy difference between the spin states of an electron. Normally degenerate, the presence of a magnetic field separates the two spin states parallel to it in energy - known as the Zeeman splitting [9]. The spin state parallel to the magnetic field has a lower energy whilst the anti-parallel state has a higher energy. These are described as the up, $|\uparrow\rangle$, and down, $|\downarrow\rangle$, spin states. For an electron in free space the energy difference is given by:

$$\Delta E = g_e \mu_b B, \tag{2.1}$$

where g_e is the free electron g-factor, μ_b is the Bohr magneton and $B$is the magnetic field strength. This results in an energy splitting as seen in figure 2.1.

In practice this energy splitting can be detected using continuous wave EPR. Transitions between the spin states will be driven by incident electromagnetic radiation of photon energy equal to the energy gap (i.e $h\nu = g_e \mu_b B$). The presence of an EPR transition in a sample can be detected either by applying a constant magnetic field and sweeping EM frequency

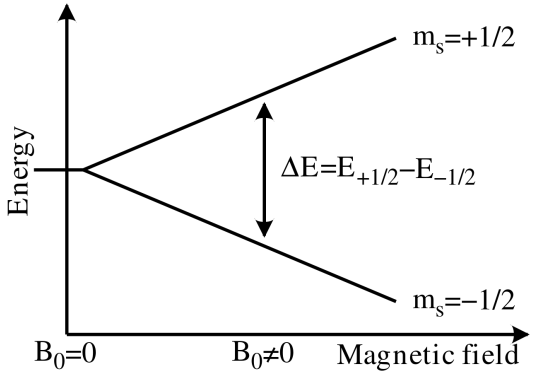

Figure 2.1: Spin state energy splitting for a free electron in a magnetic field.

incident on that sample or vice versa. In practice, it is the latter that is used for experimental simplicity. Measuring reflection of radiation from the sample whilst sweeping magnetic field will reveal a drop in reflection at the transition field - when photons are absorbed by spins moving from the lower to higher energy state.

2.1.2 Pulsed Electron Spin Resonance and Qubits

The description above details continuous wave (CW) ESR, a technique that has proven invaluable for studying the electronic structure of materials. Another ESR has proven more popular for the manipulation of spins for use of qubits: pulsed ESR. This uses short bursts of microwave radiation, on resonance with the spin transition, to control spin states and allows the spin to function as a qubit. This control is achieved by placing the spins at the centre of a cavity which produces a magnetic field when a pulse is applied. This magnetic field causes precession which can be used to rotate the spins. Pulses are described in terms of a rotation angle, with a π pulse taking the ensemble of spins from the down to up state or vice versa. A $\pi/2$ pulse takes the spins into the plane normal to the magnetic field, termed the $x-y$ plane. This causes the spins to precess in the static magnetic field at the Lamor frequency given by:

$$\omega = \frac{eg}{2m} B_0 \tag{2.2}$$

Hahn Echo and Detection

In pulsed ESR the spins are detected via the electromagnetic radiation they emit when precessing in a magnetic field. This radiation is of the same frequency as the resonant control radiation (easily shown using equations 2.1 and 2.2). This emitted radiation can be demodulated with the control radiation giving a DC signal. In a perfectly homogeneous magnetic field all spins would precess at the same rate giving a constant DC signal. In reality however, all spins will precess at slightly different rates due to small, static differences in the magnetic field each experiences. So, following a $\pi/2$ pulse, the signal from the spins will rapidly decay as the ensemble of spins lose phase coherence. A technique, known as a spin or Hahn echo, to reverse this loss of phase was developed by Erwin Hahn in 1950 [14]. This follows a $\pi/2$ pulse with a π pulse after a set time interval, T. *Static* magnetic field differences now act to reverse the loss of phase coherence. This results in a brief re-phasing of the spins following another interval T, detected as a rise and fall of a DC signal or and 'Echo'. A cartoon of this sequence is shown in figure 2.2.

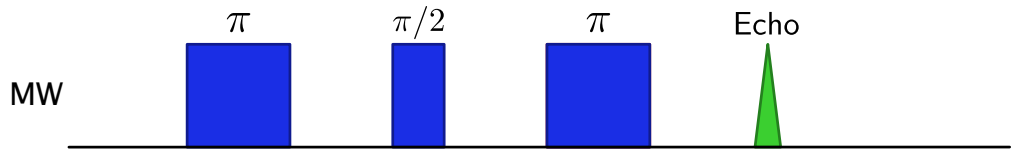

Figure 2.2: Cartoon showing a Hahn echo pulse sequence. A $\frac{\pi}{2}$ pulse causes the spins to precess in the $x-y$ plane. Loss of phase coherence is reversed via a π pulse following time interval T and a signal is detected following another interval of T.

The Bloch Sphere

The control pulses produce a magnetic field that rotates at the same rate as the spins, meaning a fixed coordinate system can be defined. The rotation axis of the control pulses can be changed by varying their phase, for example to a pulse of 0 phase is defined as a rotation about the x axis whilst a pulse of $\pi/2$ phase is a rotation about the y. This allows control of the direction of the spin vector in 3-D space, with the z-axis defined by the static magnetic field. A qubit, the basic unit of a quantum computer, can be described as a point within a unit sphere, known as a Bloch sphere and shown in figure 2.3 [17]. Clearly then, a single spin is an archetypal qubit: its eigenstates of $|\uparrow\rangle$ and $|\downarrow\rangle$ form the poles of the Bloch sphere. Microwave pulses of defined duration and phase enable the creation of an arbitrary linear superposition that allows the initialisation of any state on the surface of the Bloch sphere. In the case of ESR, however, a huge number (10^{10}) of spins is being addressed. Although this means that they do not represent a true qubit, measurements of ensemble properties give great insight into the behaviour of single spins. It is therefore prudent to establish the anticipated behaviour of the various potential spin qubit candidates using the comparatively simple experimental techniques of ESR before making the challenging step to single spin control and measurement.

2.2 Donor States in Silicon

2.2.1 The Hyperfine interaction

Discussion so far has focussed on single electrons in a magnetic field. The spins discussed in this thesis will be those of the electrons and nuclei of donors in silicon. For these spin states the situation is a little more complicated than the case of a free electron. For all the donors discussed here, there is a nuclear as well as electron spin. This introduces first an additional term in the Hamiltonian of the system due to the nuclear spin's Zeeman interaction with the magnetic field. On top of the separate Zeeman interactions there is an additional interaction

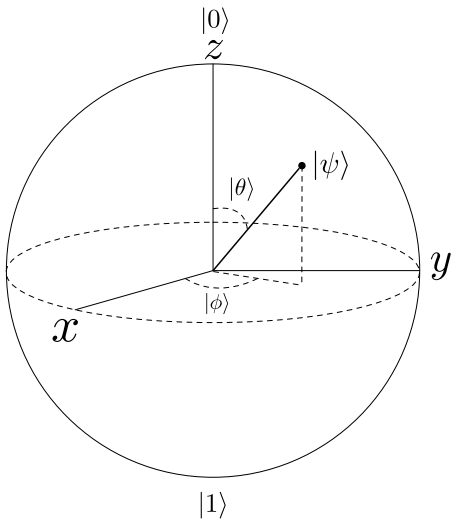

Figure 2.3: Diagram of the Bloch sphere - the most common representation of a qubit. The poles of the sphere at $\pm z$ represent the $|0\rangle$ and $|1\rangle$ or $|\uparrow\rangle$ and $|\downarrow\rangle$ states. Any point on the surface of the sphere represents some linear superposition of these two states. The state vector of any point is given by: $|\psi\rangle = \cos\theta/2\,|0\rangle + e^{i\phi}\sin\theta/2\,|1\rangle$

between the nucleus and the electron, known as the hyperfine interaction. This term is due to the magnetic field of the electron interacting with the magnetic dipole moment of the nucleus. This strength of this interaction is proportional to the overlap between the electron and nuclear wavefunctions. The result of this is that it is preferential energetically for the electron and nuclear spins to be anti-aligned. A further term in the Hamiltonian is due to the nuclear quadrupole but this effect is small enough to be neglected in this treatment. These effects leave a Hamiltonian of the following form:

$$\hat{H} = \mu_b g_e B_0 \hat{S}_z + \mu_n g_n B_0 \hat{I}_z + A\hat{S}\cdot\hat{I}, \tag{2.3}$$

where μ_b&μ_n are the Bohr and nuclear magnetons, g_e&g_n are the electron and nuclear g-factors, $\hat{S}$&$\hat{I}$ are the electron and nuclear spin operators, and A is the hyperfine interaction term. In general they hyperfine term is a tensor but due to the isotropic nature of silicon can be represented as a scalar here.

2.2.2 Spin Transitions

The electron spin is restricted to be $\pm\frac{1}{2}$, but the nuclear spin can take a much greater range of values. The nuclear spin of a phosphorus donor in silicon is $\pm\frac{1}{2}$, by contrast for a bismuth

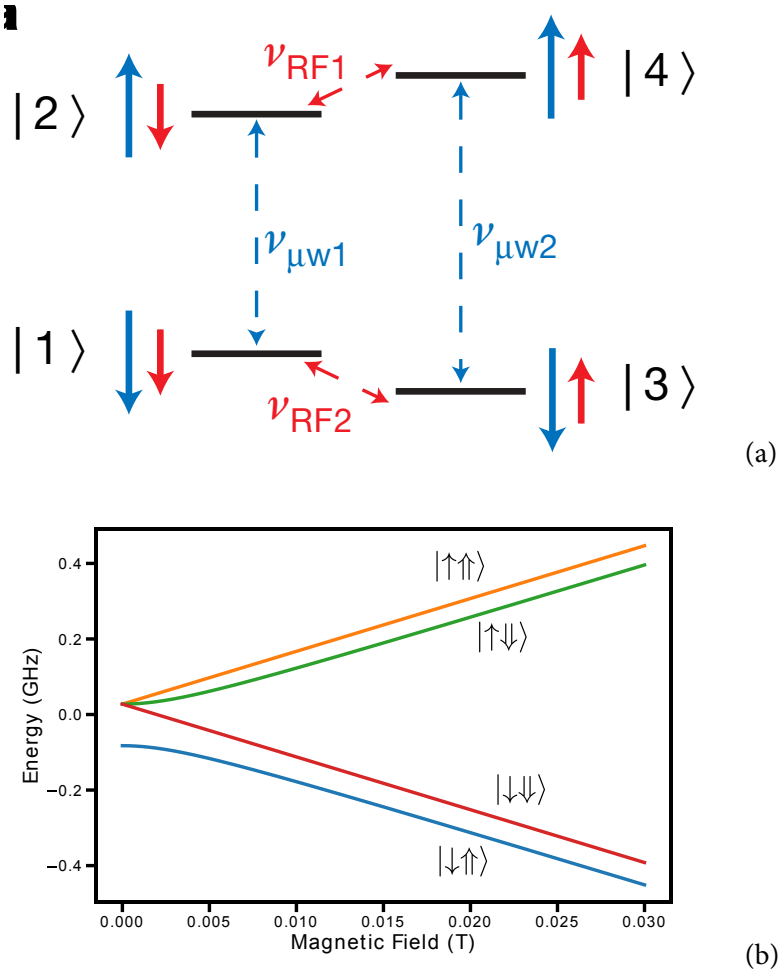

Figure 2.4: Cartoon in a shows the relative energy levels for the different spin states of phosphorus in a high field environment. Note that in this case the electron Zeeman interaction dominates the hyperfine term which dominates the nuclear Zeeman term. b shows the simulated energies for each of the four possible states of the system.

spin it can take the values $-\frac{9}{2}, -\frac{7}{2}, ...\frac{7}{2}, \frac{9}{2}$. In the simple case of phosphorus this results in the four energy levels seen in figure 2.4.

For the more complex case of bismuth, instead of 4 possible energy levels there are 20. Not all transitions are possible - spins are changed by the absorption or emission of a photon, leaving only transitions where the total spin changes by ± 1 as allowed. This means that only nuclear or electron spin can be flipped at once, not both. It should be clear that the transitions that involve an electron spin flip (e.g. $|\uparrow\Uparrow\rangle \longrightarrow |\downarrow\Uparrow\rangle$) are significantly higher in energy than those involving a nuclear spin flip (e.g. $|\uparrow\Uparrow\rangle \longrightarrow |\uparrow\Downarrow\rangle$). At typical experimental magnetic fields (≈ 0.3 Tesla), the nuclear transitions are at frequencies of 10s of MHz, whilst

the electron transitions are at ≈ 9.7 GHz. In addition to their different energies electron and nuclear transitions have different strengths or Rabi frequencies. The electron spin transition is much stronger and occurs on the order of nanoseconds at typical pulse powers, with the nuclear transition being on the order of microseconds.

2.2.3 Relaxation Processes

For spins in silicon, three main relaxation or decoherence processes occur, causing the loss of information.

Dephasing

The first of these was briefly discussed above - dephasing - the time scale for the process is termed T_2^* This is the process by which an ensemble of spins loses phase coherence due to each spin experiencing a different static magnetic field. As was described above, this loss of information can be reversed by a Hahn echo sequence.

Relaxation

The second process is known as relaxation and its time scale is termed T_1. A spin ensemble at a given temperature and magnetic field will have a Boltzmann distributed population across the available spin states defined by the magnetic field axis (i.e. across the eigenstates of the $\hat{Z}$ operator). The difference between higher and lower energy states is known as the polarisation of the ensemble. If this polarisation is reversed by a π pulse, then on a time scale T_1 it will relax back to thermal equilibrium. As this process almost always involves interaction with the silicon crystal lattice it is also termed *spin-lattice* relaxation. This process is strongly correlated with temperature and exact mechanisms will be discussed in the literature review section.

Decoherence

The third process, decoherence, occurs on the time scale T_2. This is similar to the dephasing process described above but is irreversible. Irreversible phase differences are caused by by inhomogeneous and *time dependent* magnetic fields. Additional phase acquired due to a time varying magnetic field will not be reversed by a Hahn echo sequence as the field will act differently on the spin in the second half of the sequence.

2.2.4 Summary

The theory discussed above gives a background to the topics that will be discussed in detail during the literature review section of this report.

3 Literature Review

Having introduced the background theory to the work discussed in this report, I turn to a more detailed examination of the literature surrounding this work. I begin with the various relaxation and decoherence processes for spins bound to donors in silicon. First discussing the mechanisms by which these processes occur I shall then move on to the effect of illumination on these mechanisms. Following this I shall move on the the stark shift of donor spins in silicon, including a brief introduction to the principle before an examination of previous work performed to characterise this effect in the various species of donor in silicon.

3.1 Mechanisms of Relaxation and Decoherence

The concept of T_1, T_2 and T_2^* time was introduced in section 2.2.3 as the characteristic relaxation, decoherence and dephasing respectively. I shall now focus on the established mechanisms by which these occur, looking mainly at relaxation and decoherence as these represent a permanent loss of information.

3.1.1 Relaxation

The relaxation time, T_1, determines the rate at which the polarisation of an ensemble of spins returns to Boltzmann equilibrium after being disturbed. The first method of relaxation that should be considered is spontaneous emission: the emission of a photon into free space as the spin relaxes from excited to ground state. For a magnetic dipole this rate is slow in normal circumstances - thousands of seconds or more [3, 24]. Given that above millikelvin temperatures the rate of transverse relaxation for donor spins in silicon is significantly greater than this it can be neglected as a dominant mechanism.

Spin-lattice relaxation occurs instead via the interaction with of the spin system with vibrations in the silicon lattice - phonons. There are three different phonon-mediated processes that affect the relaxation rate of spin systems with transition frequency ω_s, all of which are well described in a 1961 paper by Orbach [20, 30].

Direct Process

The first of these is a **direct process**, whereby a single phonon with frequency equal to that of the spin transition (as given by equation 2.3) is emitted into the lattice. This rate ($\propto 1/T_1$) is proportional to the phonon density at ω_s and varies with spin transition frequency and temperature as: $\omega_s^4 T^{-1}$.

Raman Process

Whilst this rate dominates at lower temperatures, < 10k, at temperatures with $k_B T \gg \hbar\omega_s$, a two phonon Raman transition becomes more efficient. As the maximum phonon density is at much higher frequencies than ω_s, the spin first absorbs a phonon at ω_{max} before emitting a phonon with $\omega = \omega_{\text{max}} + \omega_s$. This corresponds to the spin transitioning to a virtual energy level before rapidly transitioning back to the spin ground state. For non-integer spin systems the rate due to this effect scales with temperature as: T^7.

Orbach Process

The Raman process involves a virtual energy level so is an inherently off-resonant effect. It is possible for the spin to transition to an actual excited state during the two phonon process. This is known as an Orbach process and is more efficient than either process above. It scales with temperature as: $\exp(-\Delta E/K_B T) - 1$.

3.1.2 Decoherence

At high temperatures the spin-lattice relaxation rate tends to be the dominant process for spins in silicon. However, at temperatures below ≈ 10k other factors become limiting. In particular the decoherence or T_2 time becomes important. This is the process by which the spins lose phase coherence irreversibly. There are several mechanisms that contribute to T_2, detailed here.

Spectral Diffusion

The first of these is spectral diffusion and its impact is largely dependent on the sample used. In natural silicon samples there is a relatively high concentration of Spin-$\frac{1}{2}$ ^{29}Si nuclear spins ($4.7\%4$). Due to the large extent of the donor electron wavefunction, it is highly probable that a given donor will experience a hyperfine interaction with one or more of these nuclei. Although the large difference between the electron and nuclear gyromagnetic ratios prevents a state exchange or 'flip-flop' interaction, nearby pairs of ^{29}Si nuclei do have this interaction. The rate of exchange is slow, (≈ 100Hz) and will cause a change in the hyperfine interaction with any nearby donor electrons. This will cause the acquisition of phase differences between electrons over time. As these changes are time dependent they are *not* refocused by a Hahn

echo sequence [32]. In purified silicon samples this effect is reduced to the point that it is no longer the limiting factor in spin coherence.

Instantaneous Diffusion

In the first experiments on spin coherence times on purified silicon, the increase in coherence time was found to be on the order 2 fold [12]. The reason behind this limited increase was the high donor concentrations, leading to interaction between donors. Spins close enough to interact with one another will experience slightly different magnetic fields and the random nature of donor distribution leads to this effect being inhomogeneous. Once again, this will not be reversed by a Hahn echo sequence as two donors interacting with one another will both be flipped, meaning that the phase acquisition is unchanged. This effect is dependent on the concentration of donors in a sample according to:

$$\frac{1}{T_2^{\mathrm{ID}}} = C(2\pi\gamma_e)^2 \frac{\pi}{9\sqrt{3}}\mu_0\hbar, \tag{3.1}$$

where C is the donor concentration.

At concentrations useful for ESR techniques and at sufficiently low temperatures instantaneous diffusion will be a limiting factor in spin coherence times in almost all cases. One technique employed by Tyryshkin *et al*, open to ensemble based approaches such as ESR but not to single qubit control, is to use refocussing pulses of angle $< \pi$ in the Hahn echo sequence [29]. This effectively refocuses fewer spins during the Hahn echo sequence. This reduces the signal but increases T_2 time as the effect of instantaneous diffusion is suppressed by addressed spins being on average much further apart. At this point three further effects become limiting:

- *Direct T_1 Flips*: only relevant at higher temperatures when T_1 is close to the intrinsic T_2, $>$ 10k. This is the process of a single donor flipping to its ground state, thereby destroying its coherence.

- *Spectral Diffusion from donors*: the limiting factor at low temperatures $<$ 4k, this process is similar to the spectral diffusion for ^{29}Si spins. Nearby pairs of donors undergo spin exchange, causing any other nearby donors to experience a phase shift as their hyperfine coupling changes.

- *T_1 of Neighbouring Donors*: this process is important at intermediate temperatures, between 4k and 10k. At these temperatures direct T_1 flips are yet to dominate but T_1 flips of neighbouring donors can affect the magnetic field experienced by a central donor. This effect is known as T_1-type spectral diffusion. This process was identified by Tyryshkin *et al* as producing lower than expected T_2 times when T_1 ap-

peared to no longer be a limiting factor [29]. The decoherence rate as a function of T_1 induced spectral diffusion has a characteristic, stretched exponential of the form $\exp(-(2\tau/T_{SD})^2)$, with $T_2^{SD} = \sqrt{T_1}$.

The five key contributors to decoherence are shown in figure 3.1. The key contributors to decoherence times are then:

- *Temperature*: when T_1 is sufficiently short at high temperatures the T_1 of the donors will restrict T_2. At intermediate temperatures T_1 flips of neighbouring donors induces spectral diffusion, reducing T_2.
- *Sample Purity*: the concentration of ^{29}Si spins in the silicon has a significant impact on T_2 due to spectral diffusion via nuclear spin flip-flop.
- *Donor Concentration*: the concentration of donors increases the rate of instantaneous diffusion, indirect flip-flop, direct flip-flop and T_1 type spectral diffusion.

With the mechanisms of decoherence addressed, we now turn to examine the effect of illumination on donor relaxation and coherence rates.

3.2 Illumination and Decoherence

3.2.1 Free Carriers and Decoherence

The discussion above centred on the typical factors that affect coherence and relaxation times: temperature, donor concentration and silicon purity. One of the key questions addressed in this report is the impact of another factor on relaxation times: illumination. Feher and Gere were among the first to examine this impact in their 1959 paper [11], analysed using CW ESR of phosphorus donors in silicon. The key question that they examined is the impact of illumination wavelength on relaxation time, the results of which can be seen in figure 3.2. The important result here is the sharp increase in relaxation rate as the photon energies exceed that of the silicon band gap, ≈ 1.12eV. As this energy is exceeded by the photons, free carriers are created in the silicon conduction band as electrons are promoted from the valence band. These free carriers can scatter off the electrons bound to the phosphorus donors, causing them to relax via a state exchange. Feher and Gere postulate two possible processes that could cause this relaxation: the first is direct scattering of a donor electron by a free electron, whilst the second is a two stage process. They identify the second of these as dominant, due in the main to the low number of free electrons relative to donors in their experiments -

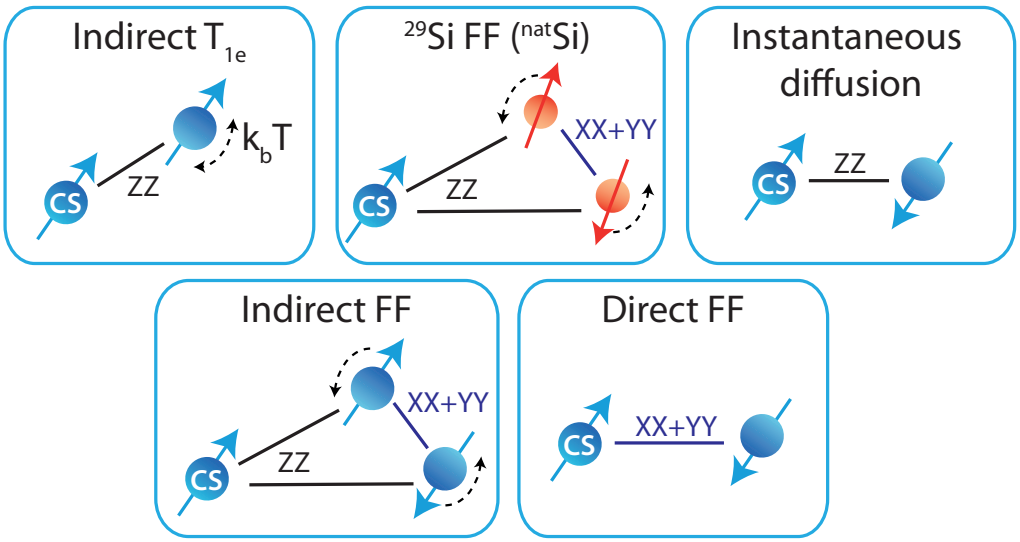

Figure 3.1: Cartoon showing the five key types of decoherence mechanisms for donor electrons in silicon. Indirect T_1 is the relaxation of a neighbouring donor modulating the magnetic field at a central donor. Flip-flops of ^{29}Si nuclear pairs modulating the magnetic field at the donor. Instantaneous diffusion is the inhomogeneous phase acquisition of donors due to different inter-donor spacings. Indirect flip-flop mechanism is similar to that involving ^{29}Si nuclei but with pairs of donors. Direct flip-flop is state exchange between a central donor and a neighbour. Figure is taken from [32].

5×10^6 vs 7×10^{15} - with each interaction requiring the subsequent relaxation of the conduction electron to the lattice. The double spin exchange process does not involve the free electron changing spin, instead both the nuclear spin of the donor and the electron bound to it change spin state. This removes the requirement that the conduction electron subsequently relax to the valence band, significantly increasing the rate of the process.

The work done by Feher and Gere was performed using only CW ESR, because of this their work addresses only the impact of laser illumination on T_1. The key timescale for quantum computing is the coherence time, T_2, which must be examined using pulsed ESR. Whilst T_2 time will ultimately be limited by T_1 a concern is that free carriers in the silicon conduction band will have an impact beyond this. It seems obvious that the presence of these free carriers could alter the magnetic environment of the donors in a time-dependent and inhomogeneous fashion, potentially having a drastic impact on the coherence time of donors. Examining the impact of illumination on decoherence times will be an important goal of this report.

Free Carrier Lifetimes

One question that is of importance is the time that free carriers will persist for following a laser pulse, as this will determine how long their effects influence relaxation and coherence times.

3.2.2 Heating and Decoherence

A potential factor not addressed by Feher and Gere is the potential impact that heating could have on relaxation and by extension coherence times. Although the number of free carriers produced by laser illumination will be significantly reduced as photon energies drop below the band gap, it is possible that heating could still have a significant impact. Of particular note is the reduced heat capacity of silicon at low temperatures. At room temperature heat capacity (C_p^o) is 19.1 J.mol^{-1}k^{-1}, but at cryogenic temperatures this is reduced by several orders of magnitude to approximately 0.004 J.mol^{-1}k^{-1} at 8k [8, 18]. Clearly then the potential impact of infra-red illumination is obvious - only a small conversion of incident photons to phonons in the lattice could potentially have a significant impact on the relaxation rates for donor spins. Exploring this potential impact will be a central goal of this report.
Having looked at some of the literature surrounding the questions of relaxation and decoherence of donors in silicon, I now move on to the stark shift of donors in silicon.

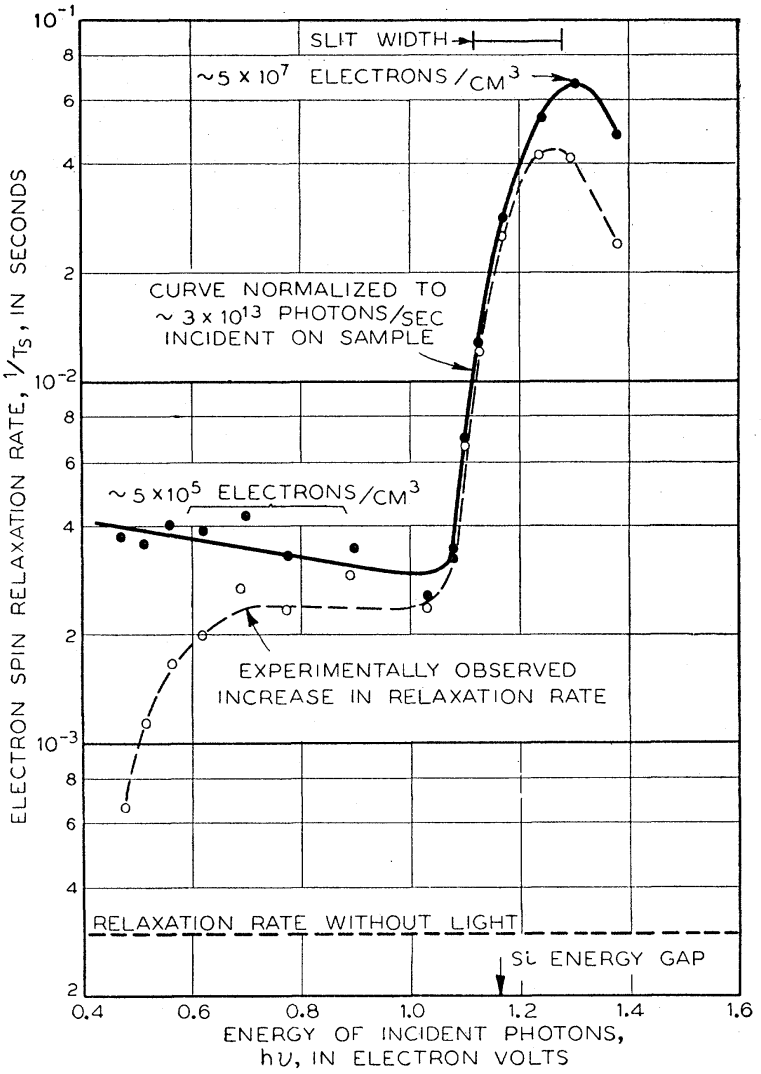

Figure 3.2: Graph from [11] showing the measured dependence of relaxation time on photon energy. Notable is the sharp increase in relaxation rate for photon energies in excess of 1.10eV. The main cause of this is that this is the energy of the photon band gap, meaning that free electrons are created in the silicon conduction band. These free electrons can then scatter off the electrons bound to donors in silicon, causing them to relax.

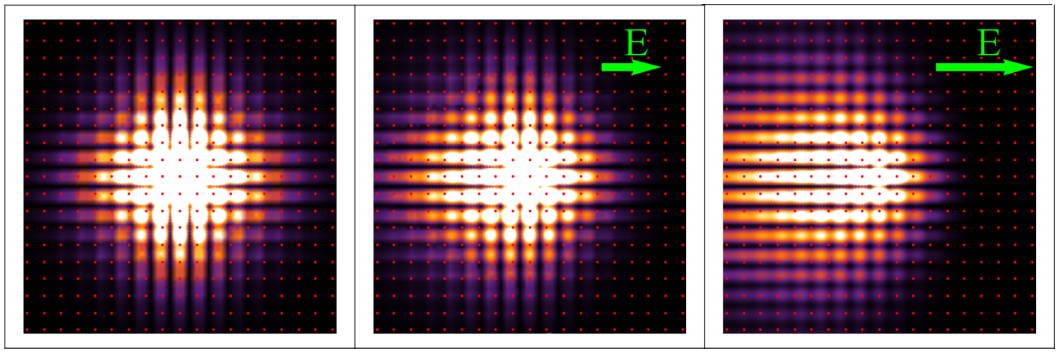

Figure 3.3: Simulation showing the density of the electron wavefunction around a donor atom. Red dots represent lattice sites. As an electric field is applied the electron wavefunction is pulled off the central site, changing the strength of its interaction with the donor nucleus and therefore its hyperfine coupling. This shifts the frequency of the electron's spin transition and its precession rate in the magnetic field. Figure reproduced from [21].

3.3 The Stark Shift

3.3.1 Introduction

The Stark shift, at its simplest, is the modulation of the hyperfine coupling between electron and nuclear spins via electric fields. The Stark shift was employed in Kane's original proposal as a means to control which qubits interact with an applied control pulse [15]. As well as the potential application for control of donor spins, the Stark shift presents a problem in the potential for electric field noise to cause decoherence of donor spins. This impact may become particularly important for single donors close to electrical contacts where distances are short and so fields high. Clearly then an understanding of the stark shift and its impact on donors is useful both from control and decoherence perspectives.

An intuitive understanding of the stark shift is easily grasped: the electron's wavefunction extends over space and is concentrated at the donor nucleus. This concentration determines the hyperfine coupling of the spin to the donor. An electric field changes this wavefunction, effectively pulling it off the nucleus and changing the hyperfine coupling, as seen in figure 3.3. This in turn changes the energy difference between the two spin states of the electron and modulates its precession frequency in a static magnetic field.

3.3.2 Theory

A technical description of the Stark shift in most cases employs effective mass theory [21]. This treats the donor system as if it were a hydrogen atom with a different mass embedded in a silicon lattice as opposed to a vacuum. This is done by replacing the electron's vacuum

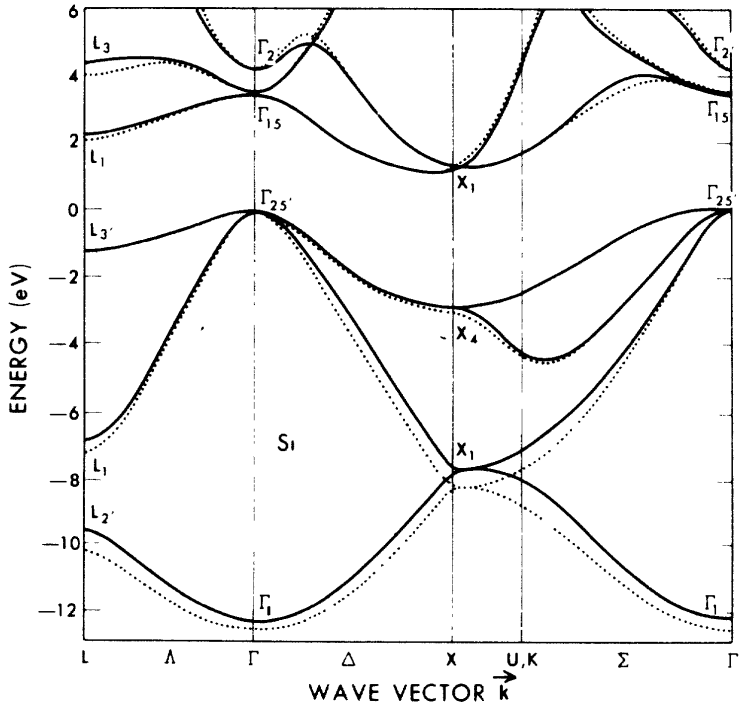

Figure 3.4: Figure from [6], showing the band structure of silicon. The top of the valence band is at Γ, the centre of the Brillouin zone, whilst the minimum of the conduction band is at X, towards the edge of the zone.

mass with its effective mass in the silicon and modifying the vacuum permittivity with the dielectric constant of silicon [32]. The conduction band of silicon has 6 minima - usually termed 'valleys' - situated in the $\pm x, \pm y, \pm z$ directions and close to the edge of the Brillouin zone, as seen in figure 3.4.

The approach of effective mass theory is to decompose the electron wavefunction into six along these conduction band valleys, giving the equation:

$$\psi(r) = \sum_{\mathrm{i}=1}^{6} \alpha_{\mathrm{i}} \phi_{\mathrm{i}}(r) F_{\mathrm{i}}(r), \tag{3.2}$$

here $\phi_{\mathrm{i}}(r) = u_{\mathrm{i}} e^{i\boldsymbol{k}_{\mathrm{i}} \cdot \boldsymbol{r}}$, the Bloch wavefunction such that $u_i(r)$ has the periodicity of the lattice and $\boldsymbol{k}_{\mathrm{i}} = k_0 \mathrm{i}$ with k_0 the momentum value at the valley minimum. In the electron ground state these valleys are six-fold degenerate, giving the singlet state [28]:

$$\text{Singlet } (1sA_1) \left\{ \boldsymbol{\alpha_g} = \tfrac{1}{\sqrt{6}}(1,1,1,1,1,1) \right. \tag{3.3}$$

This ground state is the only state with a component of the electron wavefunction at the nucleus and therefore the only one that experiences a hyperfine coupling. The excited states are as follows:

$$\text{Doublet } (1sE) \begin{cases} \boldsymbol{\alpha_r} = \frac{1}{\sqrt{12}}(-1,-1,-1,-1,2,2) \\ \boldsymbol{\alpha_s} = \frac{1}{2}(1,1,-1,-1,0,0) \end{cases} \quad \text{Triplet } (1sT_2) \begin{cases} \boldsymbol{\alpha_x} = \frac{1}{\sqrt{2}}(1,-1,0,0,0,0) \\ \boldsymbol{\alpha_y} = \frac{1}{\sqrt{2}}(0,0,1,-1,0,0) \\ \boldsymbol{\alpha_z} = \frac{1}{\sqrt{12}}(0,0,0,0,1,-1) \end{cases} \tag{3.4}$$

Bibliography

1. D. Aharonov and M. Ben-Or. "Fault-tolerant quantum computation with constant error". *Proceedings of the twenty-ninth annual ACM symposium on Theory of computing - STOC '97*, 1997, pp. 176–188. ISSN: 1533-. DOI: 10.1145/258533.258579. arXiv: 9906129v1 [arXiv:quant-ph].
2. C. J. Ballance et al. "Laser-driven quantum logic gates with precision beyond the fault-tolerant threshold". *arXiv preprint*, 2015, pp. 1–12. arXiv: 1512.04600. URL: http://arxiv.org/abs/1512.04600.
3. D. G. Baranov et al. "Modifying magnetic dipole spontaneous emission with nanophotonic structures". *Laser and Photonics Reviews* 11:3, 2017. ISSN: 18638899. DOI: 10.1002/lpor.201600268.
4. R. Barends et al. "Digital quantum simulation of fermionic models with a superconducting circuit". *Nature Communications* 6:May, 2015, p. 7654. ISSN: 2041-1723. DOI: 10.1038/ncomms8654. arXiv: 1501.07703v1. URL: http://www.nature.com/ncomms/2015/150708/ncomms8654/full/ncomms8654.html{\%}5Cnhttp://www.nature.com/doifinder/10.1038/ncomms8654.
5. S. B. Bravyi and A. Y. Kitaev. "Quantum codes on a lattice with boundary .". 96, 2008, pp. 1–6. arXiv: 9811052v1 [arXiv:quant-ph].
6. J. R. Chelikowsky and M. L. Cohen. "Electronic structure of silicon". *Physical Review B* 10:12, 1974, pp. 5095–5107. ISSN: 01631829. DOI: 10.1103/PhysRevB.10.5095. arXiv: arXiv:1011.1669v3.
7. D. J. Christle et al. "Isolated electron spins in silicon carbide with millisecond coherence times". *Nature Materials* 14:2, 2014, pp. 160–163. ISSN: 1476-1122. DOI: 10.1038/nmat4144. arXiv: 1406.7325. URL: http://www.nature.com/doifinder/10.1038/nmat4144.
8. P. D. Desai. *Thermodynamic Properties of Iron and Silicon*. 1986. DOI: 10.1063/1.555761.
9. G. Feher. "Electron spin resonance experiments on donors in silicon. I. Electronic structure of donors by the electron nuclear double resonance technique". *Physical Review* 114:5, 1959, pp. 1219–1244. ISSN: 0031899X. DOI: 10.1103/PhysRev.114.1219.
10. R. P. Feynman. "Simulating physics with computers". *International Journal of Theoretical Physics* 21:6-7, 1982, pp. 467–488. ISSN: 00207748. DOI: 10.1007/BF02650179. arXiv: 9508027 [quant-ph].

11. E Gere and G Feher. "Electron Spin Resonance Experiments on Donors in Silicon. II. Electron Spin Relaxation Effects". *Physical Review* 114:5, 1959, p. 1245. ISSN: 0031899X. DOI: 10.1103/PhysRev.114.1245.
12. J. P. Gordon and K. D. Bowers. "Microwave spin echoes from donor electrons in silicon". *Physical Review Letters* 1:10, 1958, pp. 368–370. ISSN: 00319007. DOI: 10.1103/PhysRevLett.1.368.
13. D. Gottesman. "Stabilizer Codes and Quantum Error Correction". 2008, 1997. ISSN: 0163-6804. DOI: 10.1017/CBO9781107415324.004. arXiv: 9705052 [quant-ph].
14. E. L. Hahn. "Spin Echoes". *Physical Review* 80:4, 1950, pp. 580–594.
15. B. E. Kane. "A silicon-based nuclear spin quantum computer". *Nature* 393:6681, 1998, pp. 133–137. ISSN: 0028-0836. DOI: 10.1038/30156. URL: http://www.nature.com/doifinder/10.1038/30156{\%}5Cnpapers2://publication/doi/10.1038/30156.
16. G. Q. Liu et al. "Single-Shot Readout of a Nuclear Spin Weakly Coupled to a Nitrogen-Vacancy Center at Room Temperature". *Physical Review Letters* 118:15, 2017, pp. 1–5. ISSN: 10797114. DOI: 10.1103/PhysRevLett.118.150504. arXiv: 1612.07944.
17. M. A. Nielsen and I. L. Chuang. *Quantum Computation and Quantum Information: 10th Anniversary Edition*. 10th. Cambridge University Press, New York, NY, USA, 2011. ISBN: 1107002176, 9781107002173.
18. T. O. Niinikoski et al. "Heat capacity of a silicon calorimeter at low temperatures measured by alpha-particles". *Epl* 1:10, 1986, pp. 499–504. ISSN: 12864854. DOI: 10.1209/0295-5075/1/10/003.
19. J. O'Gorman et al. "A silicon-based surface code quantum computer". *arXiv* 1:October 2015, 2014, pp. 1–11. ISSN: 2056-6387. DOI: 10.1038/npjqi.2015.19. arXiv: 1406.5149.
20. R. Orbach. "On the Theory of Spin-Lattice Relaxation in Paramagnetic Salts". *Proceedings of the Physical Society* 77:4, 1961, pp. 821–826. ISSN: 0370-1328. DOI: 10.1088/0370-1328/77/4/301.
21. G. Pica et al. "Hyperfine Stark effect of shallow donors in silicon". *Physical Review B - Condensed Matter and Materials Physics* 90:19, 2014, pp. 1–10. ISSN: 1550235X. DOI: 10.1103/PhysRevB.90.195204. arXiv: 1408.4375v1.
22. J. Preskill. "Reliable Quantum Computers", 1997, pp. 1–24. ISSN: 1364-5021. DOI: 10.1098/rspa.1998.0167. arXiv: 9705031 [quant-ph]. URL: http://arxiv.org/abs/quant-ph/9705031{\%}0Ahttp://dx.doi.org/10.1098/rspa.1998.0167.
23. M. Reagor et al. "Demonstration of Universal Parametric Entangling Gates on a Multi-Qubit Lattice", 2017, pp. 1–7. arXiv: 1706.06570. URL: http://arxiv.org/abs/1706.06570.

24. A Schweiger and G Jeschke. *Principles of Pulse Electron Paramagnetic Resonance*. Oxford University Press, 2001. ISBN: 9780198506348. URL: https://books.google.co.uk/books?id=tkvQQElkW1wC.

25. P. W. Shor. "Fault-tolerant quantum computation", 1996. ISSN: 0272-5428. DOI: 10.1109/SFCS.1996.548464. arXiv: 9605011 [quant-ph]. URL: http://arxiv.org/abs/quant-ph/9605011.

26. P. W. Shor. "Polynomial-Time Algorithms for Prime Factorization and Discrete Logarithms on a Quantum Computer *". *SIAM Journal on Computing* 26:5, 1997, pp. 1484–1509. ISSN: 0097-5397. DOI: 10.1137/S0097539795293172. arXiv: 9508027 [quant-ph].

27. P. Shor. "Algorithms for quantum computation: discrete logarithms and factoring". *Proceedings 35th Annual Symposium on Foundations of Computer Science*, 1994, pp. 124–134. ISSN: 0272-5428. DOI: 10.1109/SFCS.1994.365700.

28. G. D. J. Smit et al. "Stark effect in shallow impurities in Si". *Physical Review B - Condensed Matter and Materials Physics* 70:3, 2004, pp. 1–10. ISSN: 01631829. DOI: 10.1103/PhysRevB.70.035206. arXiv: 0310492 [cond-mat].

29. A. M. Tyryshkin et al. "Electron spin coherence exceeding seconds in high purity silicon". *Nature Materials* 11:2, 2011, p. 18. ISSN: 1476-1122. DOI: 10.1038/nmat3182. arXiv: 1105.3772. URL: http://arxiv.org/abs/1105.3772.

30. J. H. Van Vleck. "Paramagnetic relaxation times for titanium and chrome alum". *Physical Review* 57:5, 1940, pp. 426–447. ISSN: 0031899X. DOI: 10.1103/PhysRev.57.426.

31. M. Vasmer and D. E. Browne. "Universal Quantum Computing with 3D Surface Codes", 2018, pp. 1–21. arXiv: 1801.04255. URL: http://arxiv.org/abs/1801.04255.

32. G. Wolfowicz. "Quantum Control of Donor Spins in Silicon and Their Environment". PhD thesis. 2015.

33. G. Wolfowicz et al. "Atomic clock transitions in silicon-based spin qubits." *Nature nanotechnology* 8:8, 2013, pp. 561–4. ISSN: 1748-3395. DOI: 10.1038/nnano.2013.117. arXiv: 1301.6567. URL: http://www.ncbi.nlm.nih.gov/pubmed/23793304.